EB2013-MS-008-Paper

REDUCED ORDER BRAKE MODELS TO STUDY THE EFFECT ON SQUEAL OF PAD REDESIGN

[1,2]Vermot des Roches, Guillaume*, [1,2]Balmes, Etienne, [3,4]Chiello, Olivier, [5]Lorang, Xavier
[1]SDTools, France, [2]Arts et Metiers ParisTech-PIMM, France, [3]IFSTTAR-LTE, France, [4]CeLyA, France, [5]SNCF-I&R, France

KEYWORDS – structural dynamics, reduction, brake squeal, non-linear simulations, design

ABSTRACT – Brake squeal impacts trains during station parking, generating over 110 dB at the wheel vicinity. This disturbance is a problem for commuters and employees working close to trains and limits exploitation times. The only adjustable parameter is here the brake pad, since it is the only part with frequent replacement regarding the railway equipment lifetimes. To improve current pad design to limit noise emissions a numerical prototyping tool is required, providing noise level indicators post-treated from transient simulations of industrial brakes. Such realization is impossible without a relevant reduction strategy. The CMT (Component Mode Tuning) method integrated by SDTools makes this feasible. This model reduction is not only necessary to transient simulations but also to reduce the global computational cost of all intermediate operations. In the proposed approach, the pads must be kept unreduced to allow their interchangeability, but invariant brake parts can be reduced.
A reduction basis is only relevant if it provides accurate results for various configurations of a reduced parametered model. A study of the system reduction basis sensitivity must be undertaken, which is this paper main objective. A sensitivity study methodology is then proposed and results in the form of reduced model convergence are eventually presented.

INTRODUCTION

Brake squeal impacts trains during station parking operations, generating over 110dB at the wheel vicinity. This disturbance is a problem for station employees working close to trains, and commuters. It also limits train exploitation possibilities, and European regulations on train noise emissions are tightening. Brake system design is however fixed on trains due to homologation constrains and long equipment lifetime. The only adjustable parameter is here the brake pad, which needs frequent replacement. The brake pad market is then very dynamic with competition between several suppliers sharing over 30 million euros per year for the TGV (high speed train) only.

Although design of mechanical assemblies has shown dramatic evolution in the past decades, friction induced instabilities in brake systems remains unassessed. Initial engineering choices are oriented toward performance constraints that limit noise reduction solutions. The difficulty to properly model contact roughness at the structure level also prevents any simulation to be robustly predictive, however trends can be found that can orient design towards quieter brakes. Furthermore, current computational power makes accessible simulation of industrial structures. Developing a numerical prototyping procedure efficient regarding output trends and also simulation times is then the challenge undertaken by SNCF (the French railway agency) and its partners in the AcouFren project. The main objective is to provide robust noise level indicators to new pad designs before prototyping for TGV (high speed train) and a regional train. Updated brake models have been generated, presented in figure 1. These models feature between 850,000 and 1,600,000 DOF (degrees of freedom). Although numerical simulations are here available for steady sliding and complex modal analysis, computation times make direct parametric simulations impossible. Performing transient simulations, necessary to obtain non linear vibration levels is also not directly feasible.

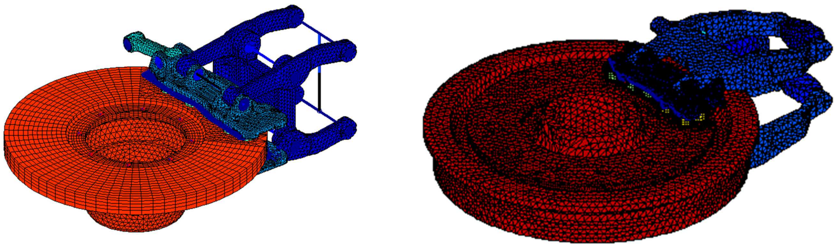

Figure 1. Industrial railway brakes. Left: the TGV brake (disc mounted on the axle), 850,000 DOF. Right: a regional train brake (disc mounted on the wheel), 1,600,000 DOF.

The CMT is a recent reduction method developed by the authors (1) that provides a very efficient framework for quick parametric studies of system redesign. Contrarily to the classical Component Mode Synthesis (CMS) methods, the full modes of a nominal configuration of the system are considered accessible. Although ambitious, this assumption is nowadays reasonable thanks to the continuous increase of computational power and the emergence of multi-level algorithms (*e.g.* AMLS eigenvalue solvers). This reduction method allows generating highly compact models with exact nominal modes. It then allows parametric setups around the nominal configuration to quickly evaluate the system behavior evolution. It was used here to generate a hybrid reduced model allowing pad switching. To ensure proper prediction over any pad design, the reduction basis may need to be enhanced.

This paper first presents the TGV brake model with its working parameters and the detailed CMT application. The full system deformations basis sensitivity to the brake parameter is then studied to choose a relevant reduction basis. The last section presents results of the reduced order model convergence.

1. THE COMPONENT MODE TUNING METHOD (CMT) AND ITS PARAMETRIZATION APPLIED TO THE TGV BRAKE

<u>The industrial TGV brake system</u>

The industrial brake studied in this paper is the main braking organ of the French high speed train (TGV), as presented in figure 1. The system itself is composed of a disc mounted on the wheel axle through a hub (rotor), and a rig fixed to the bogie (stator). The rig is composed of two levers linked by rods to the bogie that press the pads into the disc when the actuator is pressurized. 4 pads are mounted in each brake (2 by holders). On a real train, four of these systems are fitted on each wheel axle. The simulations presented in this paper focus on a single system, in accordance to the test bench configurations used by the SNCF.

Every large component of the brake system has been modelled using Finite Elements, and updated through correlation of experimental measurements. Connections in the rig and disc are represented with structural elements (beams, mass, springs, bushes) allowing to properly take into account the connection types and the mass and stiffness of the bolting. The system mechanical clearances have been fixed and a procedure has been developed to place the system in kinematic position where the pads are in zero clearance with the disc, as function of the pad height. To avoid mesh incompatibilities at the pad/disc interface, a procedure was also developed to remesh on the fly the disc section underlying the pad. Exploitation of non-compatible interfaces is possible, but must be treated with care. This was thus non desirable for the project.

The pad fixation to the rig has been simplified. It originally features a dove-tail joint fixation here represented by a stiffness elastic coupling between the surfaces of the pad backplate and the rig caliper. Such coupling is deemed sufficiently representative in effective braking configurations when the caliper presses the pad onto the disc.

Braking working points are normalized, which simplify the parameters to be retained (table 1). For an operating brake, the contact force command *Fz*, the disc angular velocity *Om*, and the friction coefficient µ must be taken into account. The main difficulty comes here from the braking pad variation, which adds the pad model *Pad*, and the elastic pad/caliper coupling coefficient *Kpg*. No link between *Pad* and *µ* exists here since µ is taken as the global resulting friction coefficient, and since wet configurations may be studied.

Pad	G1	G2	G3
Working parameters	*Min*	*Max*	*NPoints*
Fz	7.5 kN	15 kN	2
µ	0	0.8	3
Om	-4 rad/s	4 rad/s	2
Kpg	10^6 N/mm	10^{10} N/mm	2

Table 1. TGV brake retained simulation parameters (names in bold), and chosen values. Pads change the industrial brake mesh and are thus separated from other parameters. This table features 72 brake configurations

For each parameter a variation range must be chosen, as synthetized in table 1, for the reasons described in the following:

- *Pad*. Three pad designs are chosen corresponding to the project pilot pads, presented in figure 2. The first one, *G1*, is the most common one in current operating TGV trains, and consists in an assembly of 9 circular friction pins fixed to a backplate through metallic rings. The second one, *G2*, features an architecture adding flexibility to the link between its backplate and its 10 polygonal friction pins. The third one, *G3*, is of older design and features 9 cylindrical pins fixed to a robust backplate.
- *Kpg*. In braking configurations this value should be high (10^{10} N/mm) as the pad is pressed between the disc and caliper. However, low loaded areas may exist depending on the pad that justifies choosing a lower value to test.
- *Fz*. The braking force is directly commanded in the brake system. The values chosen here are the extreme values used in the squeal test bench during the project.
- *µ*. A nominal value of 0.4 was chosen as representative of the common cases. The ability to represent wet configurations and possible very harsh braking conditions, lead to consider two more values at 0 and 0.8.
- *Om*. The effect of the angular velocity amplitude is not very clear as it is indirect. Since the system is not symmetrical the sign of the angular velocity is important to consider. No other change is expected thus a value of +/- 4rad/s corresponding to a train speed of a few km/h was chosen.

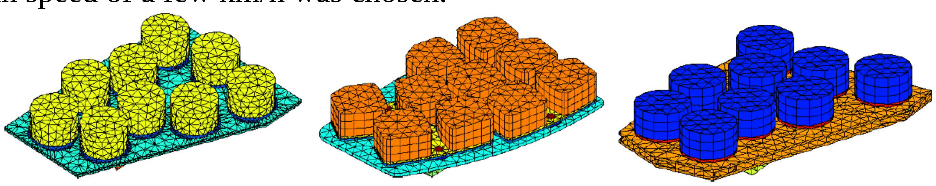

Figure 2. The pilot pads studied in this paper, from left to right, G1, G2, G3.

Decomposition of the TGV brake system for a partial reduction

The industrial brake model presented in the previous section can be decomposed into four parts (figure 3) with specific coupling between each other.

- The *brake rig*, whose displacement DOF are noted q_{rig}. The brake rig is only coupled to the pad using the parametered elastic coupling stiffness Kpg, and is invariant.
- The *pads*, whose displacement DOF are noted q_{pad}. The pads are coupled to the underlying disc area by contact displacement constraint, and to the brake rig through the elastic coupling stiffness Kpg. This part can vary.
- The *disc part candidate to contact*, whose displacement DOF are noted q_{dc}. It is coupled to the disc part outside the contact area by displacement and to the pad by contact displacement constraint. This part can vary.
- The *hub and disc outside contact*, whose displacements DOF are noted q_{do}. It is only coupled to the disc contacting area. This part is invariant.

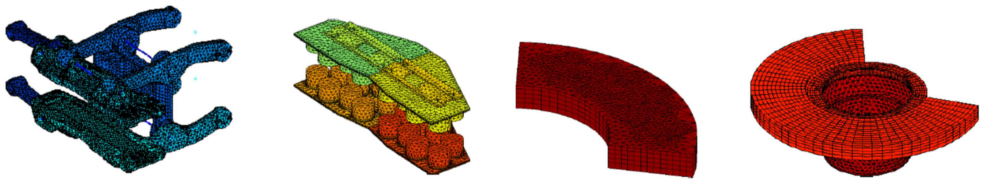

Figure 3. Brake decomposition. Left to right: rig, pads, disc candidate to contact, disc and hub outside contact.

In this formalism, the assembled brake stiffness matrix can be written

$$[K_{brake}] = \begin{bmatrix} K_{rig} & K_{pg}^T & 0 & 0 \\ K_{pg} & K_{pad} & 0 & 0 \\ 0 & 0 & K_{dc} & K_{doc}^T \\ 0 & 0 & K_{doc} & K_{do} \end{bmatrix} ; \{q_{brake}\} = \begin{Bmatrix} q_{rig} \\ q_{pad} \\ q_{dc} \\ q_{do} \end{Bmatrix} \qquad (1)$$

The reduction proposed here aims at reducing the system size in its invariant areas, *i.e.* reducing q_{rig} and q_{do}. The reduction basis used for the CMT can be conceptually formulated as a set of Rayleigh-Ritz vectors spanning a subspace of the component displacement DOF. This can be written as

$$\{q_{brake}\} = \begin{Bmatrix} q_{rig} \\ q_{pad} \\ q_{dc} \\ q_{do} \end{Bmatrix} = \begin{bmatrix} \phi_{rig} & 0 & 0 & 0 \\ 0 & \mathcal{I} & 0 & 0 \\ 0 & 0 & \mathcal{I} & 0 \\ 0 & 0 & 0 & \phi_{dc} \end{bmatrix} \begin{Bmatrix} q_{R\_rig} \\ q_{pad} \\ q_{dc} \\ q_{R\_do} \end{Bmatrix} \qquad (2)$$

where q_{R_rig} and q_{R_do} are the reduced (or generalized) DOF of respectively the rig and disc part outside contact, ϕ_{rig} a set of vectors spanning a subspace of the rig displacement, ϕ_{dc} a set of vectors spanning a subspace of the disc outside contact displacement, and $\mathcal{I}$ is the identity. Noting this reduction basis $[T_{db}]$, the reduced brake stiffness matrix writes

$$[T_{db}]^T[K_{brake}][T_{db}] = \begin{bmatrix} \phi_{rig}^T K_{rig} \phi_{rig} & \phi_{rig}^T K_{pg}^T & 0 & 0 \\ K_{pg}\phi_{rig} & K_{pad} & K_{dp}^T & 0 \\ 0 & K_{dp} & K_{dc} & K_{doc}^T \phi_{do} \\ 0 & 0 & \phi_{do}^T K_{doc} & \phi_{do}^T K_{do} \phi_{do} \end{bmatrix} \qquad (3)$$

From this *reduced database* matrix, changing the pad only requires assembling K_{pad}, K_{dc}, and the projected matrices $\phi_{rig}^T K_{pg}^T$ and $K_{doc}^T \phi_{do}$.

From the computational performance point of view, generating reduced order models is not only relevant if the system size is reduced but also if the matrix density is not too altered.

Using traditional CMS formulations, reduced component interfaces must be kept explicitly, and equation (3) would become

$$\begin{Bmatrix} q_{rig\_1} \\ q_{rig\_2} \\ q_{pad} \\ q_{dc} \\ q_{do} \end{Bmatrix} = \begin{bmatrix} \begin{bmatrix} \phi_{rig\_1} & -K_{rig\_1}^{-1}K_{rig\_12} \\ 0 & \mathcal{I} \end{bmatrix} & 0 & 0 & 0 \\ & & 0 & 0 \\ 0 & \mathcal{I} & & \\ 0 & 0 & \mathcal{I} & 0 \\ 0 & 0 & -K_{do}^{-1}K_{doc} & \phi_{dc} \end{bmatrix} \begin{Bmatrix} q_{R\_rig\_1} \\ q_{rig\_2} \\ q_{pad} \\ q_{dc} \\ q_{R\_do} \end{Bmatrix} \quad (4)$$

where the rig has to be split as a part q_{rig_1} that can be reduced and an interface q_{rig_2} coupled to the pad that cannot be reduced. The apparition of attachment modes $[-K_{rig\_1}^{-1}K_{rig\_12}]$ and $[-K_{do}^{-1}K_{doc}]$ raises issues in terms of model size. Indeed these generate potentially large full blocks in matrices, increasing with the interface size. For the TGV brake decomposed as suggested, the interfaces feature over 30,000 DOF, which would result in matrices weighting over 6.5GB each. The CMT strength is to permit an implicit reduction of these interfaces, represented by the compact form of the reduction basis (2). The resulting matrices only weight 2GB each for the models presented in section 3.

2. CHOOSING A REDUCTION BASIS FOR THE TGV BRAKE CMT MODEL

A reduction basis for steady state sliding (statics)

For statics computation, the kinematics provided by the chosen subspace must allow a proper rig and disc static deformation. The best way to realize this is to choose a family of static deformations as function of the varying parameters.

Noting $q_{brake\_p_i}$ the static displacement vector for the parameter set p_i, one chooses here the collection of system static deformation restricted to the rig and disc spanned by the parameters presented in table 1. This results in 72 different static states. In addition the attachment modes $[\psi_{brake\_b}]$ relative to the DOF loaded by the actuator are added to allow accurately representing the rig response to the load. The reduction bases used in equation (2) thus write

$$\begin{cases} \phi_{rig} = [q_{rig\_p_1} \quad \cdots \quad q_{rig\_p_{72}} \quad \psi_{rig\_b}] \\ \phi_{do} = [q_{do\_p_1} \quad \cdots \quad q_{do\_p_{72}} \quad \psi_{do\_b}] \end{cases} \quad (5)$$

Modal basis sensitivity to the retained working parameters

For dynamics computations, the complex modal bases of a new configuration must be properly approximated by the database reduction. It is here impossible to keep all the tested configurations of table 1 like in statics due to the model size. Keeping 1000 modes for each of the 72 configurations of a 1,000,000 DOF system would result in over 535 GB of data. Besides this strategy is likely to be irrelevant since a lot of redundancy should be found in this massive amount of data (*e.g.* multiple friction pin modes, with same rig deformation).

This exercise was however realized for 500 real modes in this paper study to help finding the most sensitive parameters and to illustrate the large variations of system behaviour as function of some parameters. Figure 4 presents the frequencies computed for each of the 72 configurations of the TGV brake as function of the parameters of table 1.

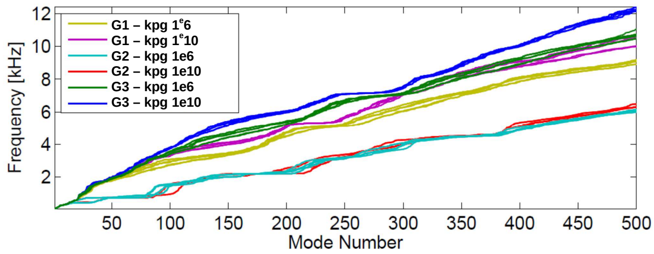

Figure 4: 500 first real modes frequencies of the 72 TGV configurations, sorted by the two most sensitive parameters.

It can be seen that depending on the parameters the frequency distribution can be drastically different. It is however clear that classes of behaviour can be distinguished. These classes are mainly dependent on the pad and the pad elastic coupling. This spread is explained by the number of local multiple friction pin modes as function of the pad. For the pad G3, the pins are stiffer and rigidly fixed to the backplate, such that only a few clusters of friction pin modes are seen. Pad G2 features a lot of local modes clusters due to its flexible fixation.

The real mode shapes computed over all configurations are rather different in a first approach. Figure 5 presents direct MAC between configurations for G1. Fz has very little impact, but Om, μ and Kpg dramatically alter the MAC diagonal.

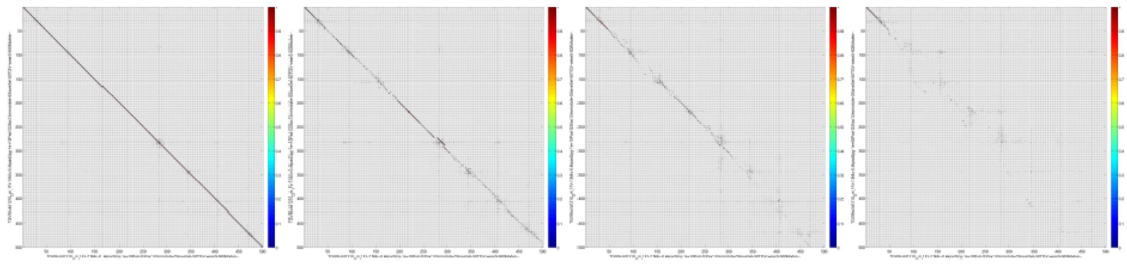

Figure 5: MAC results for the G1 pad for single parameters variations. From left to right, Fz = 7.5 to 15kN; Om = -4 to 4rad/s; μ = 0.4 to 0.8; Kpg = 10^6 to 10^{10} N/mm.

Reduction basis sensitivity and enhancement

The modal basis sensitivity seems rather drastic, but one has to keep in mind that the most influent brake part, the pad, will not be reduced. The deformation subspace variation as function of the parameters must thus be quantified component wisely. For concision matters it has been chosen to present the reduction basis study of the rig only.

To study the reduction basis sensitivity, a nominal configuration has to be chosen. The most common current TGV configuration is thus selected, and configurations for which only one parameter varies are selected as variations. 7 configurations are thus retained for this study as presented in table 2.

Configuration	*Pad*	*Om [rad/s]*	*Fz [kN]*	*μ*	*Kpg [N/mm]*
Nominal	G1	-4	7.5	0.4	10^{10}
Fz	G1	-4	15	0.4	10^{10}
Kpg	G1	-4	7.5	0.4	10^{6}
Mu	G1	-4	7.5	0.8	10^{10}
Om	G1	4	7.5	0.4	10^{10}
G2	G2	-4	7.5	0.4	10^{10}
G3	G3	-4	7.5	0.4	10^{10}

Table 2: Retained configurations to study the reduction basis sensitivity to the working parameters.

The reduction bases are obtained by restricting the fully assembled brake modeshapes to the rig. An orthonormalization has to be performed on the rig only to sort and remove redundant data from the modeshapes to generate a basis. The modeshapes orthonormalization yields a set of vectors $[\Phi_{rig}]$ such that

$$\begin{cases} [\Phi_{rig}^T][M_{rig}][\Phi_{rig}] = [\mathcal{I}] \\ [\Phi_{rig}^T][K_{rig}][\Phi_{rig}] = [\omega_j^2] \end{cases} \quad (6)$$

where $[M_{rig}]$and $[K_{rig}]$respectively are the mass and stiffness of the rig in free conditions.

Equation (6) shows that a pulsation ω_j is associated to each shape. It is linked to the energy necessary to deform the rig to get the shape. Figure 6left presents the frequencies associated to each reduction basis obtained from the modeshapes of the 7 configurations.

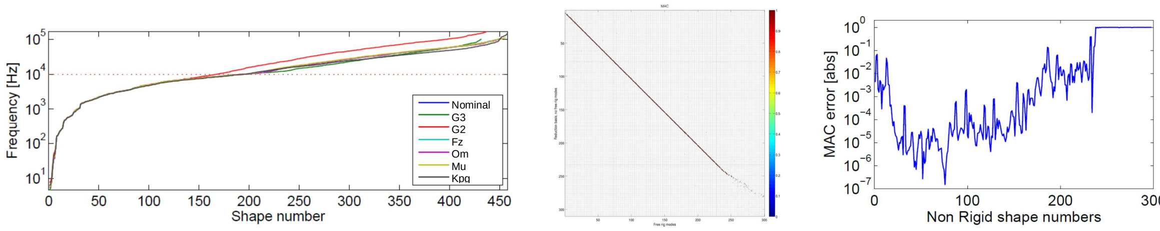

Figure 6: Frequencies associated to each orthonormalized reduction basis from the 7 retained TGV brake configurations. Left: global view. Middle: MAC computation between the orthonormalized shapes of the nominal configuration against the free brake rig modes. Right: MAC error diagonal.

Figure 6 shows two very distinct areas. A first area grouping the first 200 shapes shows very comparable frequency evolutions for all reduction bases, while for the last 300 shapes, more variations occur. Looking first at the common part, frequencies are in the order of the brake modeshape frequencies and seem rather similar. They are in fact a recombination of the free brake rig modes. The Rayleigh quotient theory explains how this is possible, and this can be verified here by computing the free rig modes and performing a MAC in figure 6middle between the orthonormalized shapes of the nominal configuration and the free rig modes. The diagonal MAC error is under 0.1 (*i.e.* a MAC of 99.9%). Thus for all reduction bases tested the free rig modes until the frequency cutoff of the modeshapes (~10kHz) are found.

In the second area of figure 6left, it can be observed that the highest frequencies are very high, which is explained by the fact that these shapes are extracted from non natural rig deformation shapes, and refer to what is commonly called enhancement (1). A way of comparing the high frequency differences is to generate a full reduction basis gathering the restricted modeshapes of all configurations, and using the orthonormalization of equation (6), corresponding results are provided in figure 7. From an original set of 3,500 full brake modeshapes, 1,546 shapes are generated. The vertical dotted lines in figure 7 illustrate the reduction basis increase due to each configuration, following the order of table 2.

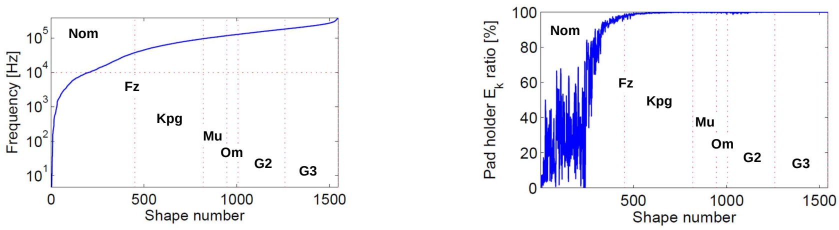

Figure 7: Left: frequencies associated to the reduction basis obtained from the concatenation of all obtained modeshapes of the 7 configurations. Right: Strain energy ratio contained in the pad holder for each shape of the reduction basis. Dotted lines show separations between configurations. Fz and Kpg lines (the first two) are overlaying (Fz had no reduction basis increase effect).

Looking at figure 7left, it can be seen that the most relevant parameters remain the pads and Kpg (Fz has no effect at all). Looking at the element strain energies associated to each shape allows understanding where the displacement information is the most sensitive. It is in fact mostly located in the pad holder. Figure 7right shows that for the free rig modes, strain energy is distributed in the rig so that the pad holder does not get over 70% of strain energy, while for enhancement shapes this ratio steeply increases from 80% to over 99%. Looking at sample reduction basis shapes in figure 8 helps visualizing where the displacement is enhanced

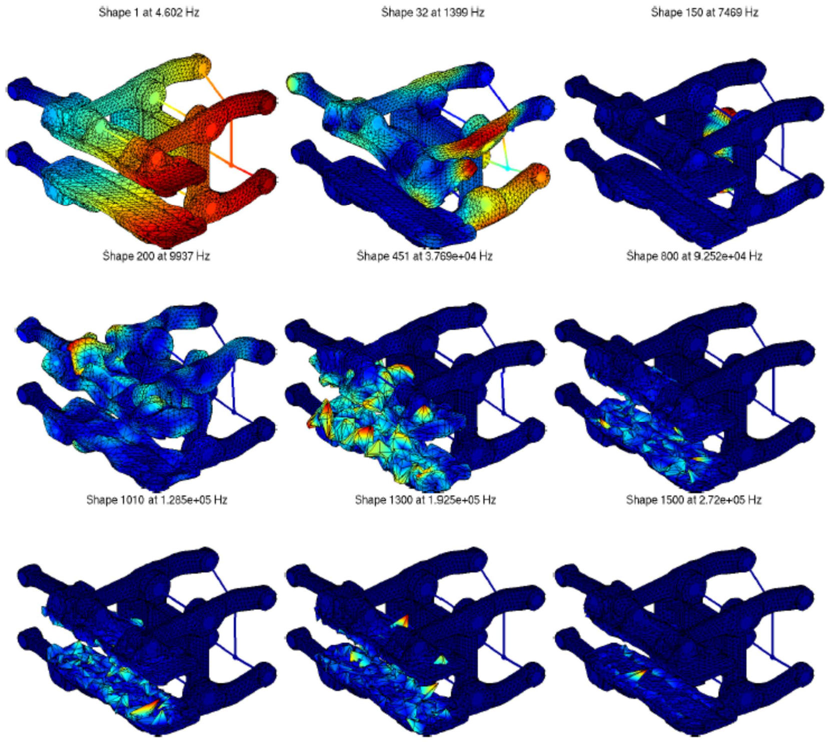

Figure 8: Sample shapes of the full orthonormalized rig reduction basis.

It seems that the best accuracy would be attained by keeping the pad holder explicitly in the model, which is impossible due to its size. Since all reduction bases generate the free rig modes under the brake frequency cutoff and provide relevant enhancement of the pad holder displacement, the first choice made is to keep the nominal reduction basis for the reduction. As a perspective, enhancement with the most different shapes (configurations with other pads) could be used. An even more efficient way of enhancing the reduction basis would also be to directly enhance looking at the local pad holder interface modes.

3. REDUCED TGV MODEL APPLICATION

The reduction method presented in section 1 is here applied with the nominal reduction basis chosen at the conclusion of section 2. All simulations presented are based on the algorithms developed for the SNCF in the PhD thesis of Lorang (2), packaged in an application tool with industrial capability based on SDT (3) and its *CMT* and *non linear simulations* modules.

Convergence of the nominal configuration

One of the main advantages of the CMT method is to provide reduced models with exact system modes for the nominal configuration. This property is also useful for transient simulation applications (1). This specific behaviour is first illustrated.

The static result error is here only presented in terms of error on the contact resultant distribution over the pads. Figure 9left shows the nominal contact resultant field. These resultants are post treated from the static deformation shape (through the stiffness matrix) and thus cannot be the most accurate due to round-off errors between heavily loaded points and slightly loaded points. Figure 9right however shows a correct prediction of the static reduced model for all contact points.

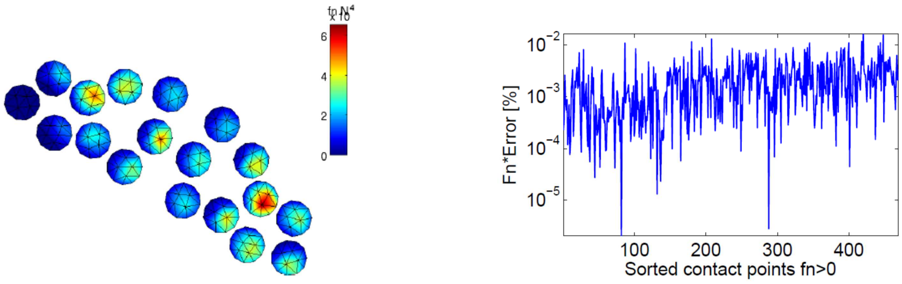

Figure 9: Model convergence in statics for the nominal configuration. Left: contact resultant distribution over the pads contact surface. Right: relative contact resultant error between the full and reduced models.

In dynamics the error on the obtained real mode basis is estimated through the frequency error computation and a MAC computation, as presented in figure 10. Figure 10left shows that the relative frequency error is under 10^{-6}% over the whole frequency range. Figure 10right shows that the MAC error diagonal is under 10^{-12} for the whole frequency band, which ensures exactitude over the numerical precision expected from a real eigenvalue solver.

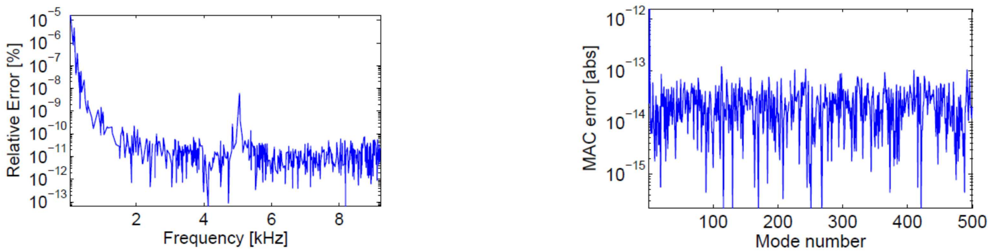

Figure 10: Model convergence in dynamics for the nominal configuration. Left: relative frequency error of the real mode basis. Right: absolute MAC error of the MAC matrix diagonal.

<u>Model convergence for non nominal configurations</u>

For each of the 72 tested configurations of table 1, the reduced model is generated using the procedure described in section 1. Results are compared to the corresponding full model. Figure 11left presents the static convergence results obtained through the comparison of post treated contact resultant fields. Depending on the pad configuration the number of pad contact points vary, which explains the relative length of each curve. It can be seen that the maximum relative error is under 0.1% which is considered acceptable.

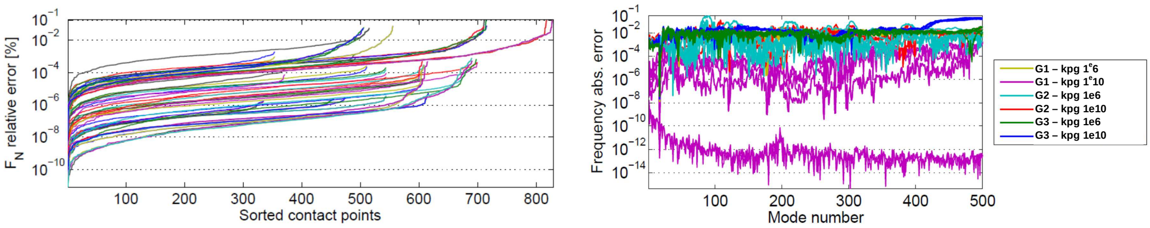

Figure 11: Left: Contact resultant relative error observed for the 72 initial configurations between the reduced static model and the full model. Right: Frequency errors of the 500 first modes of each 72 initial configurations. The configurations are classified by colours relative to the most sensitive parameters in accordance to the color code of figure 4.

Due to the round-off errors explained earlier, the higher the contact pressure the lower the error, which gives a great assurance on the result relevance. For squeal applications, lowly loaded areas do not transmit forces but are part of stick-slip areas, further investigations in the transient domain may thus be necessary.

The dynamic model validation is performed by comparing the frequency errors in figure 11right between the full and reduced models. The results obtained for the nominal configuration are the most accurate. It can be seen that predictions for variations of μ, Fz or Om are still very good. Highest errors (~10%) are found for two extreme configurations, the softest (G2, low Kpg) and the stiffest (G3, high Kpg). Investigations on these extreme cases showed that the real modes of the full stiffest configuration had some convergence issue at the solver level. A cleaner way to evaluate convergence would then be to compute FRF errors.

CONCLUSION

The ambitious aim of the AcouFren project is to deploy an industrial tool performing transient squeal simulation of industrial models for all standard braking pads. The ability to perform such computation over reasonable computers requires the distribution of reduced models with precomputed data. Such feature is now available using the CMT reduction method.

The performance of a parametered reduction method lies in its ability to span the finite element model deformation space for various and unknown future configurations. In this regard, the *a priori* choice of the reduction basis is critical. This paper provided a methodology to evaluate reduction bases sensitivity to given parameters, and possible enhancement solutions that will be undertaken later in the project.

The final objective of the simulation tool being the realization of transient simulations, a second reduction layer using the CMT again will provide the relevant results.

ACKNOWLEDGEMENTS

The authors wish to thank the members of the AcouFren project, SNCF, IFSTTAR-LTE, SDTOOLS, VIBRATEC, ENPC, ECL-LTDS, ALSTOM TRANSPORT, BOMBARDIER, FAIVELEY, and funder ADEME under the convention 0966C0281.

REFERENCES

(1) Vermot des Roches G., “Frequency and time simulation of squeal instabilities. Application to the design of industrial automotive brakes”, PhD thesis, Ecole Centrale Paris, CIFRE SDTools, 2010.

(2) Lorang X., “Instabilité vibratoire des structures en contact frottant : Application au crissement des freins de TGV”, PhD thesis, Ecole Polytechnique, 2007.

(3) Balmes E., Bianchi J.-P., Vermot des Roches G., “Structural Dynamics Toolbox 6.5 (for use with MATLAB)”, SDTools, Paris, France, www.sdtools.com, December 2012.